



# ARCHIVES of FOUNDRY ENGINEERING

 ISSN (2299-2944)  
 Volume 2022  
 Issue 3/2022

81 – 90

10.24425/afe.2022.140239

10/3

Published quarterly as the organ of the Foundry Commission of the Polish Academy of Sciences

## Impact of Values of Diffusion Coefficient on Results of Diffusion Modelling Driven by Chemical Potential Gradient

 M. Wróbel \*, A. Burbelko 

 AGH University of Science and Technology, Faculty of Foundry Engineering,  
 al. A. Mickiewicza 30, 30-059 Krakow, Poland

\* Corresponding author. E-mail address: marek.wrobel@agh.edu.pl

Received 05.05.2022; accepted in revised form 01.07.2022; available online 19.09.2022

### Abstract

In the paper critical role of including the right material parameters, as input values for computer modelling, is stressed. The presented model of diffusion, based on chemical potential gradient, in order to perform calculations, requires a parameter called mobility, which can be calculated using the diffusion coefficient. When analysing the diffusion problem, it is a common practice to assume the diffusion coefficient to be a constant within the range of temperature and chemical composition considered. By doing so the calculations are considerably simplified at the cost of the accuracy of the results. In order to make a reasoned decision, whether this simplification is desirable for particular systems and conditions, its impact on the accuracy of calculations needs to be assessed. The paper presents such evaluation by comparing results of modelling with a constant value of diffusion coefficient to results where the dependency of  $D_i$  on temperature, chemical composition or both are added. The results show how a given deviation of diffusivity is correlated with the change in the final results. Simulations were performed in a single dimension for the FCC phase in Fe-C, Fe-Si and Fe-Mn systems. Different initial compositions and temperature profiles were used.

**Keywords:** Application of information technology to the foundry industry, Diffusion modelling, Calphad, Chemical potential, Diffusion coefficient

### 1. Introduction

Finding relations for various phenomena and describing them in terms of mathematical equations in order to use them later to predict what could happen in a similar situation is a well-established approach in science. As an example can serve the problem of forecasting weather or modelling the spread of disease, both with their own journals i.e. *Weather and Forecasting* published by American Meteorological Society and *Infectious Disease Modelling* published by Elsevier B.V. where such models are shared. But these are just two of many very

complex problems that need some assumptions, drawn boundaries or simplifications to be solvable. Every numerical solution bears the risk of an error and every simplification can make that error even bigger or narrow the use of the model [1]. But using such shortcuts is not a bad thing. It is often a matter of being able to acquire some results or none at all by the means of modelling.

Simulation of diffusion process makes a very good example in the case: some results or none. It could be and was done with the use of empirical Fick's laws, where chemical composition gradient was the driving force of mass transport. For example, Fick's First Law is exact for steady state diffusion in isothermal conditions. If some process conditions differ only a little from



those restrictions then this approach still can be used to obtain modelling results that agree with the experiment within some predefined margins. However, the more conditions vary from those assumed in Fick's law, the bigger deviation of modelling results from the experimental ones may become. To ignore the limits of Fick's law, a non-simplified approach would have to be used, where mass transport is related to the gradient of chemical potential, as it is the real – correlated with the definition of equilibrium – driving force of diffusion. The ability to calculate chemical potentials, not just by obtaining the limited number of results but also by performing many calculations for ever-changing conditions in the system, was the limiting factor that prevented the use of this method. Therefore, it was preferable to obtain results with the use of methods based on chemical composition gradient, which was more or less accurate than no results at all. Nowadays the Calphad approach can be used to obtain such a big number of calculated values of chemical potentials and enables applying of methods based on chemical potential gradient. However, there is still research being done, where composition gradients are employed even in ternary systems, for example [2]. With the occurrence of the uphill diffusion in the system, considered in the mentioned paper, a mathematical trick that would change the sign of diffusion coefficient was used. This shows the supremacy of methods based on chemical potential gradients, where diffusion against composition gradient can be acquired in a straightforward way.

The presented model of diffusion, in the aspect of the driving force, is not a simplified one. It calculates fluxes using chemical potential-based equations coupled with the Calphad method to obtain up-to-date values of chemical potentials as the composition changes throughout the system during modelling time. The first results obtained using the model, that have been presented earlier [3] employed other simplification: the values of mobility and diffusion coefficient were considered constant. In this paper, the comparison of results for the constant value of diffusion coefficients versus those dependent on temperature, chemical composition or both will be assessed.

## 2. Method and theory

### 2.1. Model description

The model is based on a phenomenological flux equation that relates mass transfer to the gradient of chemical potential [4, 5].

$$J_x = -B_i c_i \frac{\partial \mu_i}{\partial x} \quad (1)$$

where  $B$  is mobility,  $c$  – composition,  $\mu$  – chemical potential. Starting with the divergence theorem and applying the Finite Difference Method (FDM) one can derive a difference equation for the change of mass for each element in the system. Such derivation was presented in previous work [3]. The final form of the equation for finite difference calculation scheme, defining change of mass for  $i$ -th element in considered cell ( $\Delta m_{0,i}$ ), for one timestep, is given by:

$$\Delta m_{0,i} = \frac{-B_{dir,i} \Delta x \Delta \tau}{2} \cdot \sum_{dir=1}^p \left[ (c_{dir,i} + c_{0,i}) (\mu_{dir,i} - \mu_{0,i}) \right] \quad (2)$$

where  $B_{dir,i}$  is the mean mobility, of  $i$ -th element, in the area between two neighbouring domains ( $dir$ , 0),  $\Delta x$ ,  $\Delta \tau$  – step in space and time,  $p$  – total number of neighbours ( $p = 2$  for 1D calculations). Indexes used in equation (2) have the form: (direction, element). Figure 1 presents exemplary values of indexes.

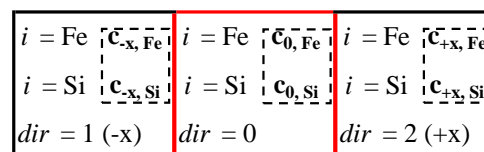


Fig. 1. Outline of FDM cell currently considered for calculations (red) together with two neighbours in 1D model. Cells contain possible values of indexes – direction “ $dir$ ”, element “ $i$ ” – and exemplary indications for composition (within the dashed frame). Integer values of  $dir$  are introduced to sum in equation (2)

Knowing the Nernst-Einstein relation that connects diffusion coefficient ( $D_i$ ) and mobility [6-8], together with  $T$  – absolute temperature and  $R$  – gas constant:

$$D_i = B_i RT \quad (3)$$

allows calculating  $B_i$  with the use of literature data for  $D_i$ . The only variable that still needs to be determined, to calculate the change in mass, is  $\mu_i$ .

As stated in [3], a very convenient way of acquiring such data is using the Calphad method. If the relation for Gibbs free energy (since in most cases this fundamental equation is available [9]) of a phase for varying values of composition and temperature is known,  $\mu$  can be calculated from the minimization of the total Gibbs energy [10]. Utilising Calphad-based software allows to calculate equilibrium and determine values of chemical potentials whether or not one has access to Gibbs free energy relations and is even more straightforward. In the presented work Thermo-Calc software (version 2019a, thermodynamic database: TCFE7) with TQ-Interface was used to obtain values of chemical potentials of each element for given conditions – temperature, composition (and constant pressure 101325 Pa).

### 2.2. Relations for diffusion coefficients and the choice of calculation parameters

It was pre-defined that the paper will present results of single dimension modelling for Fe-based binary systems. It was also decided to simulate diffusion in a single FCC phase. Literature data for diffusion coefficients was the limiting factor for the choice of systems and calculation parameters. By referring to phase diagrams (calculated using Thermo-Calc version 2019a,

thermodynamic database: TCBDIN) and analysing data for  $D_i$ , the following systems were selected: Fe-Si, Fe-Mn and Fe-C.

From the available relations of diffusion coefficients as a function of  $T$ ,  $c_i$  or both the final calculation parameters, defining modelling tasks, for each system were chosen. If  $D_i(T)$  relation was available then composition across modelled specimen was uniform and there was a linear temperature profile with  $T_{\min}$  on one edge of the specimen and  $T_{\max}$  on the other. If  $D_i(c_i)$  was found then the composition profile was linear with  $c_{\min}$  and  $c_{\max}$  on edges whereas temperature across the specimen was uniform. For the case where  $D_i(c_i, T)$  relation was available linear profiles of  $c_i$  and  $T$  with reversed slopes were used:  $c_{\min}$ ,  $T_{\max}$  on one edge and  $c_{\max}$ ,  $T_{\min}$  on another edge.

The number of space grid points was equal for each calculated system. The aim was to obtain a similar relative change of composition, in the same modelled time. For that reason, the total length of the specimen varied to reflect different values of mobility – the lower mobility the shorter specimen's length was simulated. However, for Fe-Si system it would require to use of extreme temperature gradients and though modelling allows to choose such input, it was decided to use more realistic conditions.

### 2.2.1. Fe-Si system

Figure 2 presents a fragment of Fe-Si phase diagram that covers the whole FCC area. It shows that data for diffusion coefficients should be searched roughly for temperature from the range 1000–1300°C and  $c_{\text{Si}}$  for up to 1.5 wt.%. For this system parameters for the Arrhenius relation [7], given by equation (4), were found.

$$D_i = D_0 \exp\left(\frac{-Q}{RT}\right) \quad (4)$$

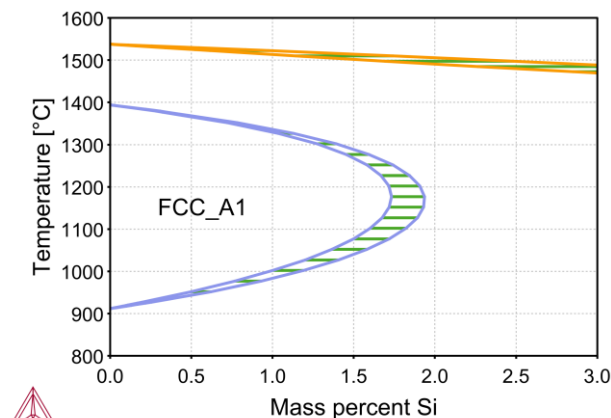


Fig. 2. Fragment of Fe-Si phase diagram covering FCC phase range

Used values of frequency factor  $D_0$  and activation energy  $Q$  in this system, within considered  $T$  and  $c_i$  limits:

For  $D_{\text{Fe}}$ :  $D_0 = 4.085 \text{ cm}^2 \cdot \text{s}^{-1}$ ,  $Q = 311.1 \text{ kJ} \cdot \text{mol}^{-1}$  [11],

For  $D_{\text{Si}}$ :  $D_0 = 0.07 \text{ cm}^2 \cdot \text{s}^{-1}$ ,  $Q = 243.0 \text{ kJ} \cdot \text{mol}^{-1}$  [12].

The above allowed to examine how adding temperature dependency to diffusion coefficients influences modelled

diffusion. The following initial conditions for modelling tasks were chosen:  $c_{\text{Si}} = 0.8 \text{ wt. \%}$ , the temperature range for  $D(T)$  1150–1250°C, the single temperature used to calculate  $D$  const.  $T = 1200^\circ\text{C}$ . The total modelled length of the specimen equals 10 mm.

### 2.2.2. Fe-Mn system

The large region of single FCC phase in Fe-Mn system, for up to 50 wt. % Mn, is presented in figure 3. It spreads throughout a huge range of temperatures and compositions.

Relations for individual diffusion coefficients, for this system, as a function of  $c_{\text{Mn}}$  (at. %) were found in [13]. Dependencies were digitalized, recalculated with respect to weight percent and approximated by polynomials. Both curves were divided into two segments for better fitting. Figure 4 presents digitalized points with polynomial approximation curves. Table 1 contains parameters of polynomials, which were used to describe relations for  $D_{\text{Fe}}(c_{\text{Mn}})$ ,  $D_{\text{Mn}}(c_{\text{Mn}})$  utilised in one of the calculation tasks.

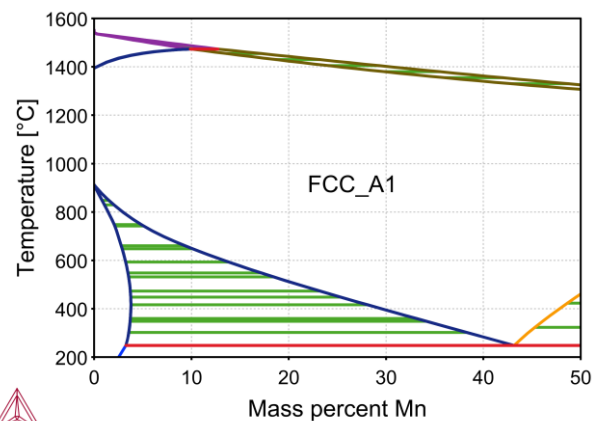


Fig. 3. Fragment of Fe-Mn phase diagram covering FCC phase range for up to 50 wt.% Mn

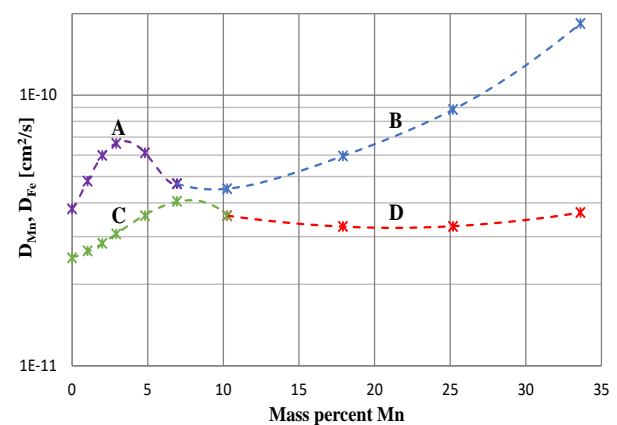


Fig. 4. Digitalised  $D_{\text{Mn}}$  (A & B) and  $D_{\text{Fe}}$  (C & D) dependencies from reference [13] (points) with polynomial approximations (curves)

Table 1.

Parameters of polynomials used to calculate values of  $D_{Fe(c_{Mn})}$  and  $D_{Mn(c_{Mn})}$

exponent	Mn		Fe	
	A	B	C	D
	$\leq 6.93$ wt. %	$> 6.93$ wt. %	$\leq 10.26$ wt. %	$> 10.26$ wt. %
4	1.489E-13	7.067E-16		
3	-1.951E-12	-4.736E-14	-5.708E-14	
2	5.681E-12	1.286E-12	6.373E-13	2.916E-14
1	6.076E-12	-1.393E-11	5.103E-13	-1.239E-12
0	3.799E-11	9.599E-11	2.521E-11	4.552E-11

Another calculation task, for single, constant values of diffusion coefficients used the data from another literature source [11]. Relation for chemical diffusion coefficient,  $\tilde{D}$ , in Fe-Mn system (for 5 at.% = 4.923 wt.% Mn,  $T = 1170^\circ\text{C}$ ) was utilised. Arrhenius equation parameters for this case are the following:

$\tilde{D}$  in Fe-Mn (5 at.%):

$$D_0 = 7.2E-2 \text{ cm}^2 \cdot \text{s}^{-1}, Q = 250.8 \text{ kJ} \cdot \text{mol}^{-1} \text{ [11]}$$

The chemical diffusion coefficient is related to the individual diffusion coefficient of species A and B in binary alloy [8] as:

$$\tilde{D} = N_A D_B + N_B D_A \quad (5)$$

where  $N_A$ ,  $N_B$  are molar fractions of two components.  $D_{Fe}$  was calculated using Arrhenius equation parameters for self diffusion of Fe, given earlier for Fe-Si system, for temperature  $1170^\circ\text{C}$ . Rewriting equation (5) gives a relation for  $D_{Mn}$ :

$$D_{Mn} = (\tilde{D} - N_{Mn} D_{Fe}) / N_{Fe} \quad (6)$$

Based on the presented data, the influence of adding composition dependency to the diffusion coefficient on the modelled diffusion was tested. The following initial conditions for modelling tasks were chosen: composition range  $0 \div 10$  wt.% Mn, temperature  $1170^\circ\text{C}$ , single Mn composition used to calculate  $D$  const:  $c_{Mn} = 5.0$  at. %. Total modelled length of specimen: 1.0 mm.

### 2.2.3. Fe-C system

Figure 5 presents a fragment of Fe-C phase diagram containing the whole FCC single phase range. Concentration and temperature dependencies of  $D_C$  in FCC iron for temperature range  $800\text{--}1100^\circ\text{C}$  and carbon concentration  $0.0 \div 1.4$  wt.% was found in [14]. The general form of this relation is given by equation (7) where  $A(T)$  and  $B(T)$  are polynomials of third degree, given by equations (8-9). Table 2 contains values of polynomials' parameters. For  $D_{Fe}$  the same temperature dependency as for Fe-Si system was used. Concentration dependency on  $D_{Fe}$  was not taken into account.

$$D_C(c_C, T) = A(T) + B(T) \cdot c_C \quad (7)$$

$$A(T) = \sum_{i=0}^3 (R_i \cdot T^i) \quad (8)$$

$$B(T) = \sum_{i=0}^3 (S_i \cdot T^i) \quad (9)$$

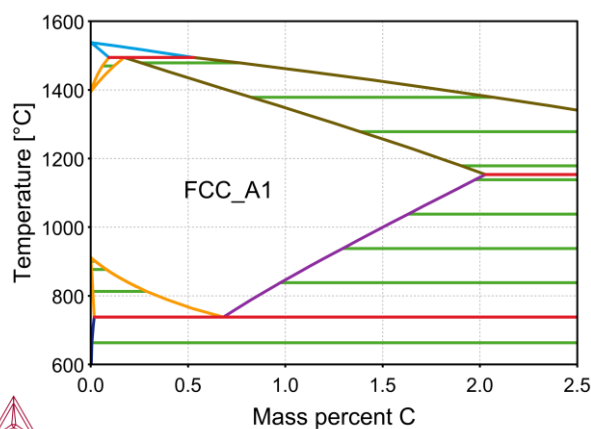


Fig. 5. Fragment of Fe-C phase diagram covering whole FCC single phase range

Table 2.

Polynomials parameters for equations (8) and (9) [14]

$i$	0	1	2	3
$R_i$	-2.69593E-5	7.41913E-8	-6.85119E-11	2.12558E-14
$S_i$	1.22170E-5	-3.20908E-8	2.78898E-11	-7.97634E-15

The data allowed to compare modelled diffusion for constant values of  $D_C$ ,  $D_{Fe}$  to three cases:  $D_C(T)$  and  $D_{Fe}(T)$ ,  $D_C(c_C)$  and  $D_{Fe}(c_C)$ ,  $D_C(T, c_C)$  and  $D_{Fe}(T, c_C)$ . Parameters for modelling tasks are the following: temperature range  $950 \div 1050^\circ\text{C}$ , single value  $T = 1000^\circ\text{C}$ , carbon concentration range  $0.5 \div 1.0$  wt.%, single value  $c_C = 0.75$  wt.%. The total modelled length of the specimen equals 50 mm.

## 3. Results

### 3.1. Fe-Si system

Table 3 contains input values defining two calculation tasks: for constant diffusion coefficients (A) and temperature-dependent one (B). Figure 6 presents the initial distribution of Si and a comparison between the modelling results after 25, 50 and 100 days for tasks A & B. Change in concentration is very low and can be observed almost only at the edges of the specimen. For that reason figure 6 presents enlarged, 1.5 mm long, segments on the margins.

Table 3.  
Parameters defining tasks A and B for Fe-Si calculations

Quantity		Value
specimen length		10 mm
temperature	$x = 0$ mm	1150°C
	$x = 10$ mm	1250°C
silicon concentration		0.80 wt. %
		Task A
		Task B
diffusion coefficient	$D_{Fe}$	single value calculated for $T = 1200^\circ\text{C}$
	$D_{Si}$	

Table 4.  
Values of Diffusion coefficients at the edges (mean temperature for task A and extreme temperatures for task B, data from ref. [11, 12]) and comparison of modelled Si composition after 25, 50 and 100 days

		$D_{Si}$		$D_{Fe}$		$c_{Si}$		$\Delta c_{Si,abs}$		$\Delta c_{Si,rel}$	
		$[\text{cm}^2 \cdot \text{s}^{-1}]$	$\frac{D_{Si,taskB}}{D_{Si,taskA}}$	$[\text{cm}^2 \cdot \text{s}^{-1}]$	$\frac{D_{Fe,taskB}}{D_{Fe,taskA}}$	[wt. %]	$\Delta c_{Si,abs}$	[wt. %]	$\Delta c_{Si,abs}$	[wt. %]	$\Delta c_{Si,rel}$
$x = 0$	task A	1.694E-10	50%	3.806E-11	41%	0.7942	1.70E-3	0.7913	2.34E-3	0.7871	3.23E-3
	task B	8.439E-11		1.559E-11		0.7959	70.6%	0.7937	72.9%	0.7903	75.0%
$x = 10$	task A	1.694E-10	192%	3.806E-11	230%	0.8058	1.90E-3	0.8087	2.57E-3	0.8130	3.44E-3
	task B	3.250E-10		8.762E-11		0.8077	132.7%	0.8113	129.4%	0.8165	126.4%

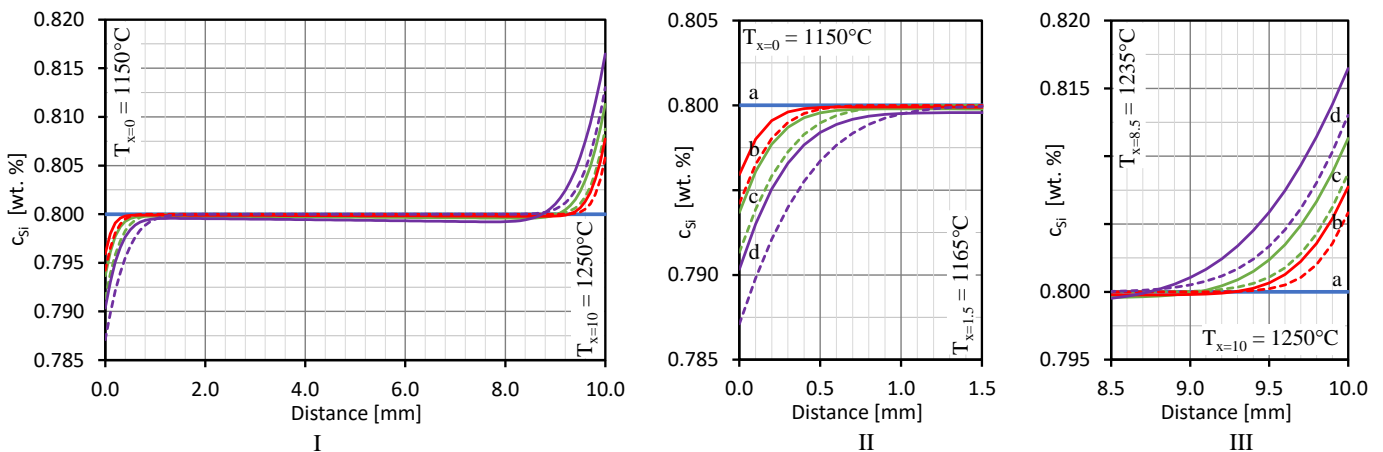


Fig. 6. Concentration profile  $c_{Si}(x)$  for the whole length of specimen (I), for 1.5 mm on the left edge (II) and for 1.5 mm on the right edge (III). Initial silicon concentration (a), and modelled distribution after: 25 days (b), 50 days (c), 100 days (d). Dashed lines: constant values of  $D_i$  – task A, solid lines:  $D_{Si}(T)$ ,  $D_{Fe}(T)$  – task B

For task A the  $c_{Si}$  curves are close to being symmetrical – after 100 days  $c_{Si}$  loss at  $x = 0$  equals 128.9E-4 wt. % whereas at  $x = 10$  mm  $c_{Si}$  gain equals to 130.3E-4 wt. %. For task B diffusion at colder edge ( $x = 0$ ) is slower than for hotter one ( $x = 10$  mm). The shape of the curves suggests that after 100 days system is still far from equilibrium and only the initial stage of diffusion has been calculated.

Within modelled 100 days absolute difference in  $c_{Si}$  at the edges between tasks A & B, calculated using equation (10), continuously increases as modelling progresses in time. Relative

change at edges calculated using equation (11), with task A being reference tents to 100%. Table 4 presents values of diffusion coefficients and absolute and relative difference in silicon concentration for  $t = 25, 50, 100$  days.

$$\Delta c_{i,abs} = c_{i,taskB}(t) - c_{i,taskA}(t) \quad \text{for } x_{min} \text{ OR } x_{max} \quad (10)$$

$$\Delta c_{i,rel} = \frac{c_{i,taskB}(t) - c_{i,taskB}(t_0)}{c_{i,taskA}(t) - c_{i,taskA}(t_0)} \quad \text{for } x_{min} \text{ OR } x_{max} \quad (11)$$

It is noteworthy that when considering the time needed for the system to reach a certain point (for example some fixed composition on the edge or at a distance from it) the differences in presented simulations are considerable. Figure 6 gives a good example showing that curve (b) for task A almost overlaps curve (c) for task B, meaning that the system needs nearly twice much time to reach the same state when employing a different approach to diffusion coefficients

### 3.2. Fe-Mn system

Table 5 contains input values defining two calculation tasks: for constant diffusion coefficient (A) and concentration-dependent one (B). Figure 7 presents the initial distribution of Mn and a comparison between modelling results after 25, 50 and 100 days for tasks A & B.

The difference between tasks A and B at  $x = 0$  mm is close to zero whereas on the other edge ( $x = 1.0$  mm) this difference is much bigger (factor of 10 for  $t = 100$  days) with faster diffusion for task A. Close to the middle of specimen we observe higher values of  $c_{Mn}$  for task A.

Table 7 presents the initial values of diffusion coefficients and the absolute and relative difference in manganese concentration for  $t = 25, 50, 100$  days. In the presented system diffusion coefficients for task B change in time – they are being recalculated for updated  $c_{Mn}$  values during modelling. At  $x = 0$  initially  $c_{Mn}$  is higher for task A, between  $t = 50$  and 100 days however due to increase of  $D_i$ , manganese concentration for task B becomes greater:  $\Delta c_{Mn, rel}$  crosses 100%, probably to reach a maximum but at  $t = 100$  days it still slowly increases. At  $x = 1.0$  mm there is also an increase of  $D_i$  for task B but  $D_{Mn}$  stays lower than the coefficient for task A and  $\Delta c_{Mn, rel}$  tends to 100%.

Table 5.  
Parameters defining tasks A and B for Fe-Mn calculations

Quantity	Value
specimen length	1 mm
temperature	1170°C
manganese concentration	$x = 0$ mm 0.0 wt. % $x = 1$ mm 10.0 wt. %
	Task A      Task B
diffusion coefficient	$D_{Fe}$ single value calculated for $T = 1170^\circ\text{C}$ dependent on $c_{Mn}$ $D_{Mn}$ single value calculated for $c_{Mn} = 5$ at. %

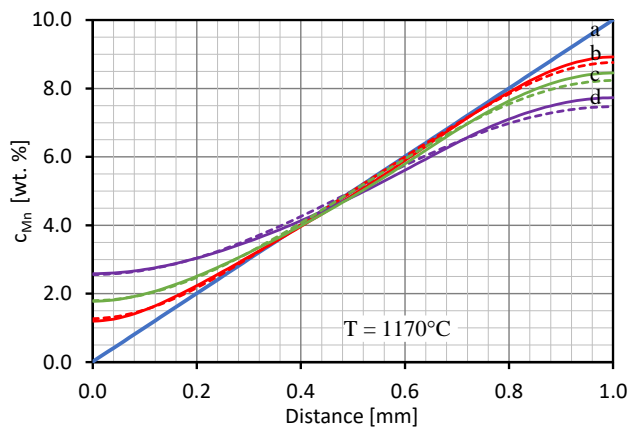


Fig. 7. Initial manganese concentration (a), and modelled distribution after: 25 days (b), 50 days (c), 100 days (d). Dashed lines: constant values of  $D_i$  – task A, solid lines:  $D_{Mn}(c_{Mn})$ ,  $D_{Fe}(c_{Mn})$  – task B

### 3.3. Fe-C system

#### 3.3.1. Constant $D_i$ versus $D_C(cc)$ and constant $D_{Fe}$

Table 6 contains input values defining two calculation tasks: for constant diffusion coefficients (A) and concentration-dependent  $D_C$  with constant  $D_{Fe}$  (B). Figure 8 presents the initial distribution of C and a comparison between modelling results after 25, 50 and 100 days for tasks A & B.

Table 6.  
Parameters defining tasks A and B for Fe-C calculations ( $D_C(cc)$ )

Quantity	Value
specimen length	50 mm
temperature	1000°C
carbon concentration	$x = 0$ mm 0.5 wt. % $x = 50$ mm 1.0 wt. %
	Task A      Task B
diffusion coefficient	$D_{Fe}$ single value calculated for $T = 1000^\circ\text{C}$ dependent on $c_C$ $D_C$ single value calculated for $c_C = 0.75$ at. %

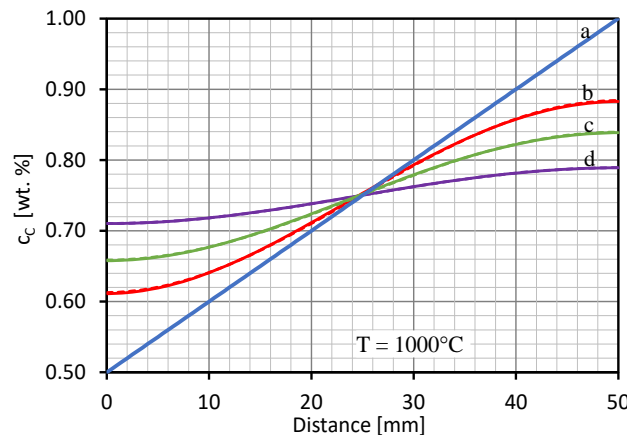


Fig. 8. Initial carbon concentration (a), and modelled distribution after: 25 days (b), 50 days (c), 100 days (d). Dashed lines: constant values of  $D_i$  – task A, solid lines:  $D_C(cc)$ ,  $D_{Fe}$  const. – task B

Table 7.

Initial values of diffusion coefficients at the edges (task A: 5 at. % Mn, data from ref. [11], task B: extreme Mn compositions, data from ref. [13]) and comparison of modelled Mn composition after 25, 50 and 100 days

		$t = 25$ days				$t = 50$ days				$t = 100$ days	
		$D_{Mn}$ [ $cm^2 \cdot s^{-1}$ ]	$\frac{D_{Mn,taskB}}{D_{Mn,taskA}}$	$D_{Fe}$ [ $cm^2 \cdot s^{-1}$ ]	$\frac{D_{Fe,taskB}}{D_{Fe,taskA}}$	$c_{Mn}$ [wt. %]	$\frac{\Delta c_{Mn,abs}}{\Delta c_{Mn,rel}}$	$c_{Mn}$ [wt. %]	$\frac{\Delta c_{Mn,abs}}{\Delta c_{Mn,rel}}$	$c_{Mn}$ [wt. %]	$\frac{\Delta c_{Mn,abs}}{\Delta c_{Mn,rel}}$
$x = 0$	task A	6.222E-11	61%	2.245E-11	112%	1.2688	-7.64E-2	1.7947	-2.13E-2	2.5584	2.35E-2
	task B	3.799E-11	$\frac{104\%}{t = 100 \text{ days}}$	2.521E-11	$\frac{133\%}{t = 100 \text{ days}}$	1.1923	94.0%	1.7734	98.8%	2.5819	100.9%
$x = 1$	task A	6.222E-11	72%	2.245E-11	165%	8.7623	1.65E-1	8.2374	2.21E-1	7.4720	2.60E-1
	task B	4.499E-11	$\frac{74\%}{t = 100 \text{ days}}$	3.696E-11	$\frac{182\%}{t = 100 \text{ days}}$	8.9277	86.6%	8.4583	87.5%	7.7322	89.7%

Table 8.

Initial values of diffusion coefficients at the edges (mean composition for task A and extreme  $cc$  for task B, data from ref. [11, 14]) and comparison of modelled C composition after 25, 50 and 100 days

		$t = 25$ days				$t = 50$ days				$t = 100$ days	
		$D_C$ [ $cm^2 \cdot s^{-1}$ ]	$\frac{D_{C,taskB}}{D_{C,taskA}}$	$D_{Fe}$ [ $cm^2 \cdot s^{-1}$ ]	$\frac{D_{Fe,taskB}}{D_{Fe,taskA}}$	$cc$ [wt. %]	$\frac{\Delta cc_{abs}}{\Delta cc_{rel}}$	$cc$ [wt. %]	$\frac{\Delta cc_{abs}}{\Delta cc_{rel}}$	$cc$ [wt. %]	$\frac{\Delta cc_{abs}}{\Delta cc_{rel}}$
$x = 0$	task A	3.907E-07	93%	7.042E-13	100%	0.6127	-1.55E-3	0.6586	-9.33E-4	0.7103	-1.95E-4
	task B	3.640E-07	$\frac{98.9\%}{t = 100 \text{ days}}$	7.042E-13	100%	0.6111	98.6%	0.6576	99.4%	0.7101	99.9%
$x = 50$	task A	3.907E-07	107%	7.042E-13	100%	0.8842	-1.47E-3	0.8395	-9.06E-4	0.7892	-2.17E-4
	task B	4.175E-07	$\frac{101.1\%}{t = 100 \text{ days}}$	7.042E-13	100%	0.8827	101.3%	0.8386	100.6%	0.7890	100.1%

The difference between tasks A and B for all three presented modelling times, throughout the entire specimen length, is very low. At the edges, there is 0.25 wt. % difference between  $cc$ , used to calculate  $D_C$ , for two tasks and this causes 7% difference in the carbon diffusion coefficient. Since the coefficient for task B is being recalculated for updated values of carbon composition  $D_C(cc)$  tends to values of task A. For  $t = 25$  days there is still 1.4%  $\Delta c_{c,rel}$  at  $x = 0$ . Table 8 presents the initial values of diffusion coefficients and the absolute and relative difference in carbon concentration, according to equations (10) and (11), for  $t = 25, 50, 100$  days.

### 3.3.2. Constant $D_i$ versus $D_i(T)$

Table 9 contains input values defining two calculation tasks: for constant diffusion coefficients (A) and temperature-dependent  $D_i$  (B). Figure 9 presents the initial distribution of C and a comparison between modelling results after 25, 50 and 100 days for tasks A & B. Similarly to Fe-Si system  $cc$  is lower for task B in the middle of the specimen and higher on the edges. Diffusion for temperature-dependent coefficients is again faster for higher temperatures and slower for lower.

Table 9.

Parameters defining tasks A and B for Fe-C calculations ( $D_i(T)$ )			
Quantity		Value	
specimen length		50 mm	
temperature	$x = 0$ mm	950°C	
	$x = 50$ mm	1050°C	
carbon concentration		0.75 wt. %	
		Task A	Task B
diffusion coefficient	$D_{Fe}$	single value	dependent on $T$
	$D_C$	calculated for $T = 1000^\circ\text{C}$	

The difference between tasks A and B, both absolute and relative, is the biggest (for presented data) for  $t = 25$  days. Table 10 contains initial values of diffusion coefficients and the absolute and relative difference in carbon concentration, according to equations (10) and (11), for  $t = 25, 50, 100$  days. At the edges, there is 50°C difference in temperature used to calculate  $D_i$  for two tasks. it causes a much bigger difference in  $D_i$  then in the previous simulation and consequently greater differences in modelled  $c_c$  between two tasks.

Table 10.

Values of Diffusion coefficients at the edges (mean temperature for task A and extreme temperatures for task B, data from ref [11, 14]) and comparison of modelled C composition after 25, 50 and 100 days

		$t = 25$ days		$t = 50$ days		$t = 100$ days					
		$D_C$ [ $\text{cm}^2 \cdot \text{s}^{-1}$ ]	$\frac{D_{C,\text{taskB}}}{D_{C,\text{taskA}}}$	$D_{Fe}$ [ $\text{cm}^2 \cdot \text{s}^{-1}$ ]	$\frac{D_{Fe,\text{taskB}}}{D_{Fe,\text{taskA}}}$	$cc$ [wt. %]	$\frac{\Delta cc_{abs}}{\Delta cc_{rel}}$	$cc$ [wt. %]	$\frac{\Delta cc_{abs}}{\Delta cc_{rel}}$	$cc$ [wt. %]	$\frac{\Delta cc_{abs}}{\Delta cc_{rel}}$
$x = 0$	task A	3.907E-07	65%	7.042E-13	30%	0.6598	8.34E-3	0.6256	7.11E-3	0.5876	3.81E-3
	task B	2.554E-07		2.118E-13		0.6681	90.8%	0.6327	94.3%	0.5914	97.7%
$x = 50$	task A	3.907E-07	148%	7.042E-13	304%	0.8456	7.74E-3	0.8849	5.65E-3	0.9292	2.10E-3
	task B	5.797E-07		2.138E-12		0.8534	108.1%	0.8906	104.2%	0.9313	101.2%

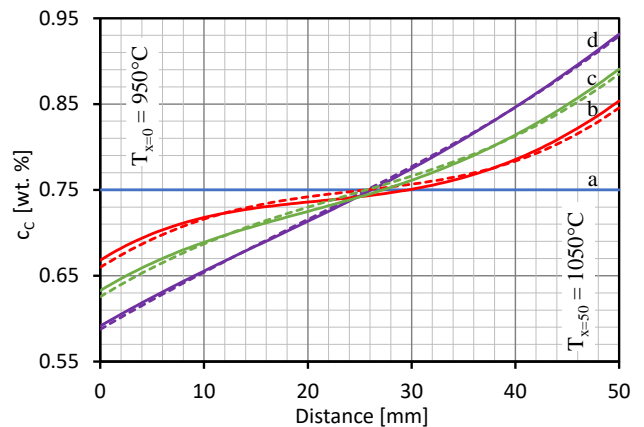


Fig. 9. Initial carbon concentration (a), and modelled distribution after: 25 days (b), 50 days (c), 100 days (d). Dashed lines: constant values of  $D_i$  – task A, solid lines:  $D_i(T)$  – task B

### 3.3.3. Constant $D_i$ vs $D_C(cc, T)$ and $D_{Fe}(T)$

Since, as presented in 0, carbon diffuses to the hotter edge, having the initial composition and temperature gradient in the same direction would mean that system is already quite close to equilibrium. To obtain bigger values of change in composition, and simultaneously have composition impact on diffusion coefficient (rejection of initial uniform composition) the composition gradient has been reversed – the higher value of  $cc$  is located at edge  $x = 0$  whereas lower at  $x = 50$  mm.

Table 11 contains input values defining two calculation tasks: for constant diffusion coefficients (A) and  $D_C(cc, T)$  with  $D_{Fe}(T)$  (B). Figure 10 presents the initial distribution of C and a comparison between modelling results after 25, 50 and 100 days for tasks A & B.

Table 11.

Parameters defining tasks A and B for Fe-C calculations ( $D_c(cc, T)$ )

Quantity	Value
specimen length	50 mm
temperature	$x = 0$ mm 950°C
	$x = 50$ mm 1050°C
carbon concentration	$x = 0$ mm 1.0 wt. %
	$x = 50$ mm 0.5 wt. %
diffusion coefficient	Task A $D_{Fe}$ single value calculated for $T = 1000^\circ\text{C}$
	Task B $D_C$ dependent on $T$
diffusion coefficient	Task A $D_C$ Single value calculated for $cc = 0.75$ wt. %
	Task B $D_C$ dependent on $cc, T$

The fastest diffusion closer to the edges causes the composition profile to have two extremes for significant simulation time (curves b and c in fig. 10). Initially, a bigger relative difference between tasks A and B can be observed for a hotter edge,  $x = 50$  mm: for  $t = 25$  days deviation from 100% is still higher there. In later stages, however, composition equalises

Table 12.

Values of diffusion coefficients at the edges (mean temperature and composition for task A and extreme temperature and composition for task B, data from ref [11, 14]) and comparison of modelled  $cc$  after 25, 50 and 100 days

		$t = 25$ days		$t = 50$ days		$t = 100$ days					
		$D_C$ [ $\text{cm}^2 \cdot \text{s}^{-1}$ ]	$\frac{D_{C,\text{taskB}}}{D_{C,\text{taskA}}}$	$D_{Fe}$ [ $\text{cm}^2 \cdot \text{s}^{-1}$ ]	$\frac{D_{Fe,\text{taskB}}}{D_{Fe,\text{taskA}}}$	$cc$ [wt. %]	$\frac{\Delta cc_{abs}}{\Delta cc_{rel}}$	$cc$ [wt. %]	$\frac{\Delta cc_{abs}}{\Delta cc_{rel}}$	$cc$ [wt. %]	$\frac{\Delta cc_{abs}}{\Delta cc_{rel}}$
$x = 0$	task A	3.907E-07	71%	7.042E-13	30%	0.7848	1.61E-2	0.7079	1.45E-2	0.6235	8.75E-3
	task B	2.791E-07	$\frac{62.5\%}{t = 100 \text{ days}}$	2.118E-13		0.8008	92.5%	0.7224	95.0%	0.6322	97.7%
$x = 50$	task A	3.907E-07	142%	7.042E-13	304%	0.6984	1.55E-2	0.7865	1.23E-2	0.8871	5.10E-3
	task B	5.531E-07	$\frac{152.2\%}{t = 100 \text{ days}}$	2.138E-12		0.7139	107.8%	0.7989	104.3%	0.8922	101.3%

## 4. Conclusions

At the beginning of each simulation, the system is the furthest from equilibrium and the driving force of diffusion (gradient of chemical potentials) is at its maximum. For that reason, the biggest difference in modelled composition, for the varying approach to the calculation of diffusion coefficients, can be found in these early stages. Since each system tends to equilibrium at its own pace, the duration of that period should be identified with the amount of mass already transferred rather than elapsed time.

For simulations that are concluded during the early diffusion (example of Fe-Si system), taking into account temperature or composition dependency on diffusion coefficient is strongly

faster on that edge due to being closer to equilibrium and the value of  $D_c$  being even higher than initially, because of its composition dependency.

Table 12 presents initial values of diffusion coefficients and the absolute and relative difference in carbon concentration, according to equations (10) and (11), for  $t = 25, 50$ , and 100 days.

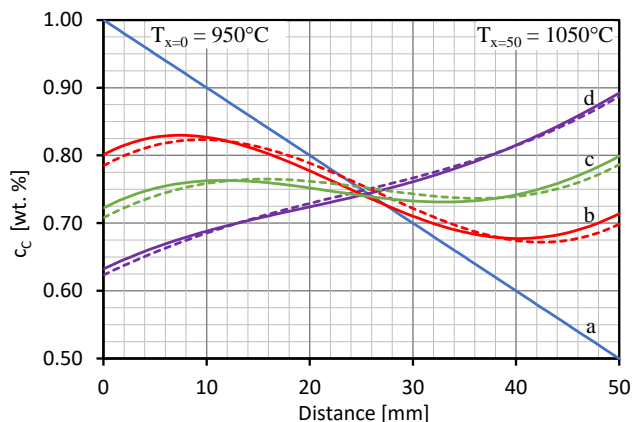


Fig. 10. Initial carbon concentration (a), and modelled distribution after: 25 days (b), 50 days (c), 100 days (d). Dashed lines: constant values of  $D_i$  – task A, solid lines:  $D_c(cc, T)$ ,  $D_{Fe}(T)$  – task B

recommended. In later stages, when the flux is getting smaller as the driving force tends to zero, the difference between the two modelling tasks slowly vanishes. For simulations that would be performed well beyond the initial stage, when the system approaches equilibrium (simulated 100 days of Fe-C diffusion), the use of the constant diffusivity simplification in the model is desirable. For cases in between (examples of Fe-Mn and modelled 25 or 50 days of Fe-C systems), the decision about the way of determining  $D_i$  should be made according to the current requirements: simplicity or accuracy of the model. The results show that the smaller the difference between constant and varying diffusion coefficient is the faster the system reaches the point when the distinction in results between two approaches becomes

insignificant. Tabularised data give a clue what is the correlation of this difference with results after a given simulation time.

The approach of using a gradient of chemical potential instead of chemical composition, as a driving force of diffusion, proves to give genuine results. It enables the calculation of segregation of alloying elements in systems exposed to non-uniform temperature field—uphill diffusion. The results for binaries are also a milestone for further expansion of the model into ternary and higher-order systems, where the addition of another element may significantly affect chemical potential and thus diffusion, making composition gradient-based models inadequate.

## References

- [1] Lambers, J.V. & Sumner, A.C. (2016). *Explorations in Numerical Analysis*. World Scientific Publishing.
- [2] Nishibata, T., Kohtake, T. & Kajihara, M. (2020). Kinetic analysis of uphill diffusion of carbon in austenite phase of low-carbon steels. *Materials Transactions*. 61(5), 909-918. DOI: 10.2320/matertrans.MT-M2019255.
- [3] Wróbel, M., & Burbelko, A. (2022). A diffusion model of binary systems controlled by chemical potential gradient. *Journal of Casting & Materials Engineering*. 6(2), 39-44. DOI: 10.7494/jcme.2022.6.2.39.
- [4] Porter, D.A., Easterling, K.E. & Sherif, M.Y. (2009). *Phase transformations in metals and alloys*. Boca Raton: CRC Press.
- [5] Bhadeshia, H.K.D.H. (2021). Course MP6: Kinetics & Microstructure Modelling. University of Cambridge.
- Retrieved July 23 2021 from: <https://www.phase-trans.msm.cam.ac.uk/teaching.html>
- [6] Bergethon, P.R. & Simons, E.R. (1990). *Biophysical Chemistry: Molecules to Membranes*. New York: Springer-Verlag. DOI: 10.1007/978-1-4612-3270-4
- [7] Shewmon, P. (2016). *Diffusion in Solids*. Cham: Springer International Publishers
- [8] Mehrer, H. (2007). *Diffusion in Solids: Fundamentals, Methods, Materials, Diffusion-Controlled Processes*. Berlin – Heidelberg: Springer-Verlag
- [9] Hillert, M. (2008). *Phase Equilibria, Phase Diagrams and Phase Transformations*. Cambridge: Cambridge University Press.
- [10] Lukas, H.L., Fries, S.G. & Sundman, B. (2007). *Computational Thermodynamics*. Cambridge: Cambridge University Press.
- [11] Brandes, E.A. & Brook, G.B. (Eds.) (1998). *Smithells Metals Reference Book. 7<sup>th</sup> Edition*. Oxford: Elsevier.
- [12] Bergner, D., Khaddour, Y. & Lorx, S. (1989). Diffusion of Si in bcc- and fcc-Fe. *Defect and Diffusion Forum*. 66-69, 1407-1412. DOI: 10.4028/www.scientific.net/DDF.66-69.1407.
- [13] Nohara, K. & Hirano, K. (1973). Self-diffusion and Interdiffusion in  $\gamma$  solid solutions of the iron-manganese system. *Journal of the Japan Institute of Metals*. 37(1), 51-61. [https://doi.org/10.2320/jinstmet1952.37.1\\_51](https://doi.org/10.2320/jinstmet1952.37.1_51)
- [14] Gegner, J. (2006). Concentration- and temperature-dependent diffusion coefficient of carbon in FCC iron mathematically derived from literature data. In the 4th Int Conf Mathematical Modeling and Computer Simulation of Materials Technologies, Ariel, College of Judea and Samaria.